ECCOMAS Congress 2016
VII European Congress on Computational Methods in Applied Sciences and Engineering
M. Papadrakakis, V. Papadopoulos, G. Stefanou, V. Plevris (eds.)
Crete Island, Greece, 5–10 June 2016

MESO-SCALE MODELING OF HYBRID INDUSTRIAL/RECYCLED STEEL FIBER-REINFORCED CONCRETE

Antonio Caggiano[1], Diego Said Schicchi[2], Guillermo Etse[1] and Enzo Martinelli[3]

[1] CONICET and Universities of Buenos Aires and Tucuman
e-mail: acaggiano@fi.uba.ar, getse@herrera.unt.edu.ar

[2] Stiftung Institut für Werkstofftechnik (IWT), Bremen, Germany
and Instituto Nacional de Tecnología Industrial, Buenos Aires, Argentina
schicchi@iwt.uni-bremen.de

[3] University of Salerno
Fisciano, Salerno, Italy
e.martinelli@unisa.it

Keywords: HyFRC, Meso-scale, Discrete Crack Approach, Zero-thickness Interface, Embedded Short Beams, Pull-out.

Abstract. *This paper investigates the mechanical behavior of fiber-reinforced concrete (FRC) and focusses on the quantifying the effect of replacing Industrial Steel Fibers (ISFs), commonly adopted as spread reinforcement in FRC, with Recycled Steel Fibers (RSFs) recovered from waste tires. More specifically, it analyses the bending behavior of FRC beams reinforced with a constant volume fraction of steel fibers and variable proportions of ISFs and RSFs. First, a numerical model is formulated by assuming that FRC behaves as a multi-phase medium, where the nonlinear material behavior of the concrete matrix is simulated by following a discrete-crack approach for meso-scale analysis. Then, steel fibers are modeled as short cables, randomly distributed and embedded within the concrete matrix. The internal forces in the steel fibers are obtained by considering both bond-slip behavior and dowel effect. Comparisons between experimental results, obtained by the authors in a previous study, and numerical simulations, performed by means of the proposed numerical model, are discussed: the significant predictive capability of the latter confirms the soundness of the mechanical assumptions on which the model is based. Moreover, the possibility of predicting the behavior of FRC with Hybrid Recycled/Industrial Fibers paves the way toward the actual application of this sustainable material in real applications. Finally, it is worth highlighting that the theoretical formulation proposed in this work stems out of the activities foreseen by the SUPERCONCRETE Project (H2020-MSCA-RISE-2014 – n. 645704), funded by the European Union as part of the H2020 Programme.*

1 INTRODUCTION

In recent years the disposal of exhaust tires has emerged as a big issue in waste management and the increasing amount of this waste actually represents a serious threat for both environment preservation and human health [1]. Based on the ‘‘Council Directive 1999/31/EC’’ of the European Commission on the Landfill of Waste, as of 2003 post-consumer ‘‘whole tires’’ could no longer be landfilled and, since July 2006, such regulations must be applied to both ‘‘whole’’ and ‘‘shredded’’ tires [2]. Therefore, there are strong motivations for recycling waste tires, which can easily be turned into an eco-friendly source of secondary raw materials.

Recycling processes of waste tires mainly consist of separating the internal steel reinforcement from the rubber covering. Rubber scraps and short steel fibers are obtained via these processes and, among other alternative solutions, they can be employed in partial-to-total replacement of ordinary concrete constituents. Particularly, rubber scraps find an interesting field of application as a partial replacement of ordinary stone aggregates for obtaining the so-called rubberized concretes [3][4]. Furthermore, Recycled Steel Fibers (RSFs) can replace Industrial Steel Fibers (RSFs) for producing a cementitious composite generally referred to as Recycled Steel Fiber Reinforced Concretes (RSFRCs) [5][6].

Various experimental studies available in the scientific literature deal with the mechanical characterization of FRC in post-cracking range. Several recently issued works have investigated the mechanical performance and the post-cracking response of the most common composite materials, i.e., Steel-FRC [7], Polypropylene FRC [8] or Hybrid-FRC [9]. Furthermore, some experimental campaigns on “ecofriendly fiber reinforced concrete composites”, such as those made with either recycled steel fibers obtained from waste tires (RSFRC) [10] or natural fibers (NFRC) [11] are also available in literature.

Several theoretical models, intended to simulate the failure behavior and post-cracking response of FRC at both material and structural levels, are also available in the literature. They range from empirical design relationships [12][13] to more complex meso-mechanical models [14][15]. The latter take into account explicitly the interaction among the different phases of the composite (i.e., fibers, matrix, coarse aggregates and their interfaces) [16] and, hence, they require a sound knowledge of fiber-matrix interaction [17][18].

This work proposes a meso-scale model aimed at simulating the failure behavior and post-cracking response of Hybrid Industrial/Recycled Steel Fiber-Reinforced Concretes (HyIRSFRCs). More specifically, a zero-thickness interface model for plain concrete is employed in the framework of a meso-scale discrete-crack approach. This discontinuous model assumes the fracture-based model originally proposed by Carol et al. [19]. Moreover, a novel and promising approach to account for the fiber effect in concrete composites and mortar has been proposed in this paper. Particularly, this new advanced extension deals with the assumption that Industrial Steel Fibers (ISFs) and Recycled Steel Fibers (RSFs) can be considered as embedded short beams randomly distributed within the concrete matrix.

The paper is organized as follows. Section 2 reports the main assumptions of the FRC modeling and approaches. After this, Section 3 describes the fracture energy-based plasticity formulation for plain mortar/concrete interfaces while Section 4 highlights the fiber bond-slip formulation and dowel mechanisms for the embedded beams. Section 5 shows a relevant application of the proposed model aimed at simulating the post-cracking response of the HyIRSFRC. Finally, some concluding remarks are given in Section 6.

2 OUTLINE OF THE MODELING APPROACH

The present model for FRC is inspired to a discrete-crack approach and considers fibers as beam elements "embedded" within the concrete matrix. Hence, it includes three internal formulations as follows:

i. *A fracture energy-based plasticity formulation for plain mortar/concrete joints*: the constitutive model for iso-parametric interface elements relates normal and tangential stress components with the corresponding relative displacements; the three-parameter hyperbolic failure surface by Carol et al. [19] is assumed as maximum strength criterion, while the ratio between fracture work and energy controls the post-cracking response: Section 3 reports further details on this model;

ii. *Fiber bond-slip* developed in the fiber (beam) direction. Pull-out mechanisms of steel fibers crossing cracks (these latter represented through opened joints) is formulated by means of an elastoplastic model as indicated in Section 4;

iii. *Fiber dowel action* based on elastic foundation concepts to obtain the dowel force-displacement relationship developed in the transversal direction of the considered short beam which crosses an active fracture: this model is detailed in Section 5.

3 FRACTURE ENERGY-BASED INTERFACE PLASTICITY FORMULATION

This section presents a rate-independent fracture-based model for concrete interfaces: Table 1 summarizes its main features, whereas further details are available in the literature [20].

	Fracture - based energy interface model
Constitutive relationships	$\dot{\mathbf{u}} = \dot{\mathbf{u}}^{el} + \dot{\mathbf{u}}^{cr}$ $\dot{\mathbf{u}}^{el} = \mathbf{C}^{-1} \cdot \dot{\mathbf{t}}$ $\dot{\mathbf{t}} = \mathbf{C} \cdot \left(\dot{\mathbf{u}} - \dot{\mathbf{u}}^{cr}\right)$
Yield condition	$f\left(\mathbf{t}, \kappa\right) = \sigma_T^2 - (c - \sigma_N \tan\phi)^2 + (c - \chi \tan\phi)^2$
Flow rule	$\dot{\mathbf{u}}^{cr} = \dot{\lambda}\mathbf{m}$ $\mathbf{m} = \mathbf{A} \cdot \mathbf{n}$
Cracking work-evolution	$\dot{\kappa} = \dot{w}_{cr}$ $\dot{w}_{cr} = \sigma_N \cdot \dot{u}^{cr} + \sigma_T \cdot \dot{v}^{cr} \qquad \sigma_N \geq 0$ $\dot{w}_{cr} = \left[\sigma_T - \lvert\sigma_N\rvert tan(\phi)\right] \cdot \dot{v}^{cr} \qquad \sigma_N < 0$
Evolution law	$p_i = \left(1 - \left(1 - r_{pi}\right) S[\xi_{p_i}]\right) p_{0i}$
Kuhn - Tucker loading/unloading and consistency conditions	$\dot{\lambda} \geq 0, \quad f \leq 0, \quad \dot{\lambda} f = 0$ **Kuhn-Tucker** $\dot{f} = 0$ **Consistency**

Table 1: Overview of the interface model for plain concrete and mortars.

In Table 1, **C** defines the uncoupled normal/tangential elastic stiffness matrix, $\dot{\mathbf{u}}^{el}$ and $\dot{\mathbf{u}}^{cr}$ the vectors of the elastic and cracking displacement rate (according to the non-associated flow rule), respectively, $f\left(\mathbf{t}, \kappa\right)$ is the hyperbola defining the yield condition of the model on the bases of the three-parameters (Figure 1) χ (the tensile strength), c (the cohesion) and ϕ (the friction angle) [19].

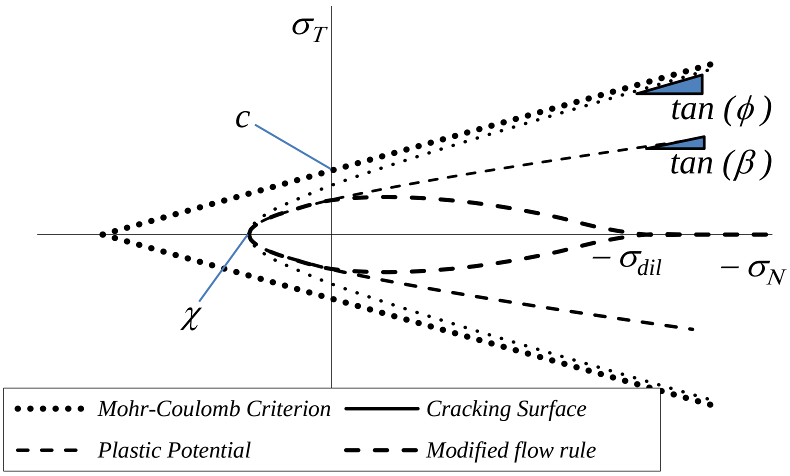

Figure 1: Failure hyperbola by Carol et al. [19], Mohr–Coulomb surface, plastic potential and modified flow rule.

The cracking displacement rate, $\dot{\mathbf{u}}^{cr} = \left[\dot{u}^{cr}, \dot{v}^{cr}\right]^t$ (where $\dot{u}^{cr}$ and $\dot{v}^{cr}$ represent the normal and the tangential components, respectively, while t interprets the transposition vector operator), is given through a general non-associated flow rule which controls the direction, **m**, of the interface fracture displacements by means of the transformation matrix operator **A** applied to the associated normal flow derivate, **n**; $\dot{\lambda}$ is the non-negative plastic multiplier derived by means of the Kuhn-Tucker loading/unloading and consistency conditions.

Furthermore, Table 1 highlights the incremental fracture work, $\dot{w}_{cr}$, which controls the evolution of the yielding surface in a generic fracture (post-elastic) process. A unified decay function is considered for each internal parameter, p_i (alternatively equals to χ, c or $\tan\phi$), of the yield condition: p_{0i} represents the initial value for p_i, $r_p p_{0i}$ the residual one and $S[\xi_{p_i}]$ the scaling function where ξ_{p_i} measures the ratio between the current work spent and the available fracture energies in mode I and II.

4 EMBEDDED SHORT BEAMS: PULL-OUT AND DOWEL EFFECTS

FRC is modeled as a meso-scale medium composed by one homogeneous matrix (aggregates and paste) plus another “phase” represented by the steel fibers. Hence, the fracture process is modeled through interface elements, in the framework of a discrete crack approach, while the stress transferred between cracks, due to fibers bridging effect, is modelled with embedded cable (beam) elements. The spatial position and orientation of fibers are generated randomly in a two-dimensional finite element mesh. The number of fibers is calculated as a function of volume fraction and geometric characteristics of the analyzed reinforcement. Then, the contributions of the steel fibers are considered through two sub-models. Two plasticity-based models are employed for modelling the fibers bond-slip behavior and dowel mechanism, respectively, in the axial and transversal direction of the fiber.

4.1 Bond-slip

This section deals with the proposed one-dimensional plasticity model for the stress-strain response. The model deals with a resulting bilinear stress-strain (σ_f–ε_N) rule which models the fiber bond–slip response (Table 2). It is based on the additive decomposition of the total strain rate $\dot{\varepsilon}_N$ into elastic $\dot{\varepsilon}_N^{el}$ and plastic $\dot{\varepsilon}_N^{pl}$ components. $\dot{\sigma}_f$ is the total stress rate while E_f represents the uniaxial elastic modulus which considers both the uniaxial response of the steel fiber and the bond-slip effect of the short steel reinforcement in mortar/concrete substrate; f_f is the yield condition, being $\sigma_{y,f}$ the initial yield stress and Q_f the internal softening variable in post-elastic regime. The evolution law is defined in terms of the incremental plastic multiplier $\dot{\lambda}_f$ and the softening module H_f.

	1D bond-slip model
Constitutive relationships	$\dot{\varepsilon}_N = \dot{\varepsilon}_N^{el} + \dot{\varepsilon}_N^{pl}$ $\dot{\sigma}_f = E_f(\dot{\varepsilon}_N - \dot{\varepsilon}_N^{pl})$
Yield condition	$f_f = \lvert\sigma_f\rvert - (\sigma_{y,f} + Q_f) \le 0$
Flow rule	$\dot{\varepsilon}_N^{pl} = \dot{\lambda}_f \partial f_f / \partial\sigma_f = \dot{\lambda}_f sign[\sigma_f]$
Evolution law	$\dot{Q}_f = \dot{\lambda}_f H_f$
Kuhn - Tucker loading/unloading and consistency conditions	$\dot{\lambda}_f \ge 0,\ f_f(\sigma_f, Q_f) \le 0,\ \dot{\lambda}_f f_f(\sigma_f, Q_f) = 0$ $\dot{f}_f(\sigma_f, Q_f) = 0$

Table 2: 1D bond-slip model.

The complete derivation of this numerical model and its validation against bond-slip experimental tests are proposed in previous works published by the authors [17][21].

4.2 Dowel action

A numerical sub-model for the dowel action has been accounted defining both stiffness and strength of the generic fiber embedded in the concrete matrix and subjected to a possible transverse force/displacement at the fracture level. The well-known Winkler beam theory is used to describe the dowel force-displacement relationship, which transformed in terms of dowel stress vs. relative displacement, allows to describing the equivalent shear beam stiffness. Further details of the numerical model for dowel mechanisms can be found in [21].

5 NUMERICAL SIMULATIONS

The simulations of 150×150×600 mm^3 pre-cracked concrete beams tested under four-point bending according to Martinelli et al. [10] are performed. Specimens of various mixtures, characterized by the same volume fraction of fibers, but different proportions of industrial and recycled reinforcements were tested in bending. The specimens presented a vertical notch (of approximately 2.0 mm wide) at the bottom (mid-length) of the beam characterized by a depth of about 45 mm. The actual beam span length is 450 mm (Figure 2).

Four FRC mixtures have been analyzed, always using 0.5% of fibers in volume of matrix plus a reference concrete without reinforcements, and also combining the aforementioned ISFs and RSFs:

- Plain concrete.
- RSFRC 0-05: with only ISFs (RSFs = 0%).
- RSFRC 50-05: with 50% of ISFs replaced by an equal amount of RSFs.
- RSFRC 100-05: with all RSFs.

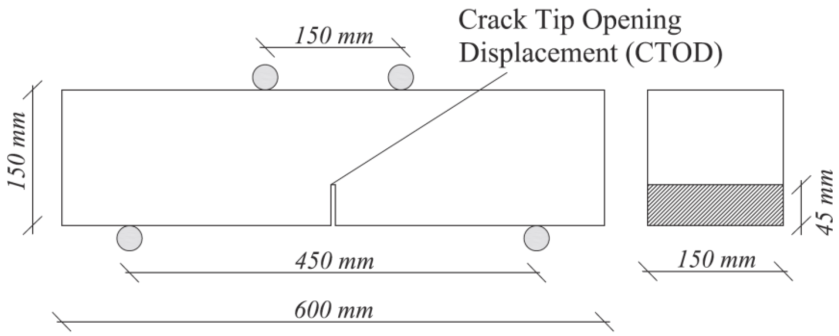

Figure 2: Geometry of the notched beam tested in four-point bending.

The explicit mesoscopic geometry is determined by means of a random 2D generation of both ISFs and RSFs as shown in Figure 3.

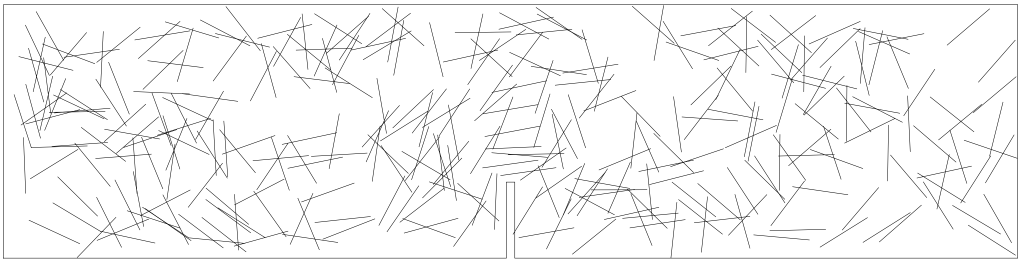

(a) RSFRC 0-05: number of ISFs=316, fiber length ISF=33 mm, diameter ISF=0.55 mm.

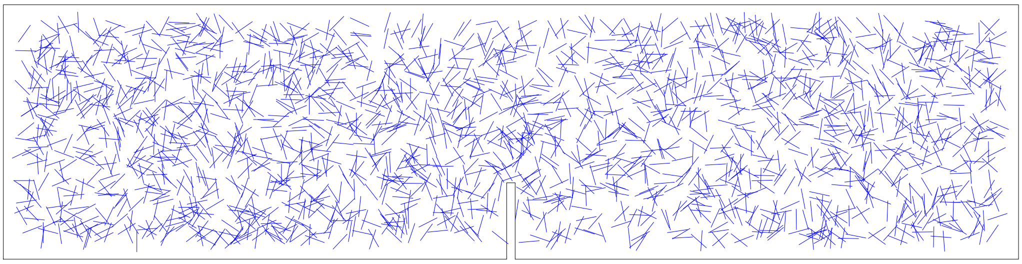

(b) RSFRC 100-05: number of RSFs=2076, fiber length (mean value) RSF=12 mm, diameter (mean value) RSF=0.23 mm [10].

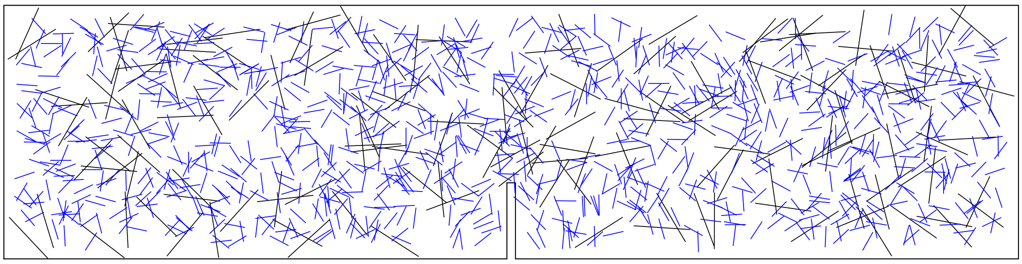

(c) RSFRC 50-05: number of ISFs=158, of RSFs=1038.

Figure 3: Two-dimensional finite element geometry: concrete phases and fibers as embedded short beams.

Figure 4 reports the 2-D geometry of the considered structure and highlights the FE discretization employed in the analyses. Plane stress hypothesis and displacement-based control are assumed. Moreover, 3-node linear elastic plane stress elements have been adopted in the FE mesh, whereas all non-linearities are concentrated within zero-thickness interface elements defined throughout the adjacent edges of the finite elements in the notch zone. Non-linear fracture-based law was introduced in those interface elements according to the formulation outlined in Section 3. Then, the constitutive models for considering the stress transferred between cracks through embedded beam elements are outlined in Section 4.

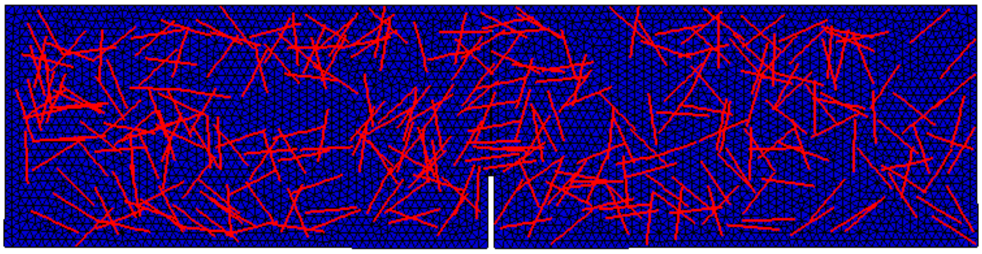

(a) Adopted FE mesh;

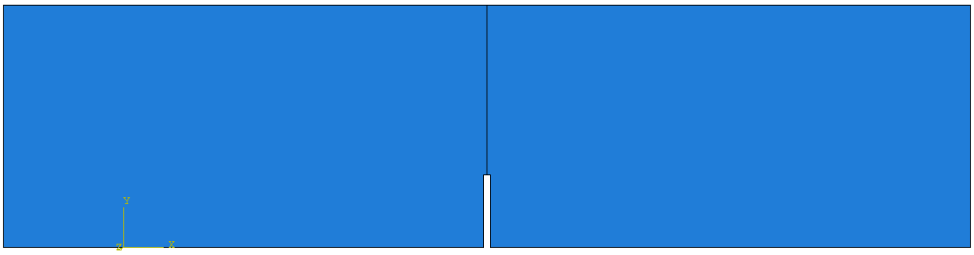

(b) Interface zone at the notch section;

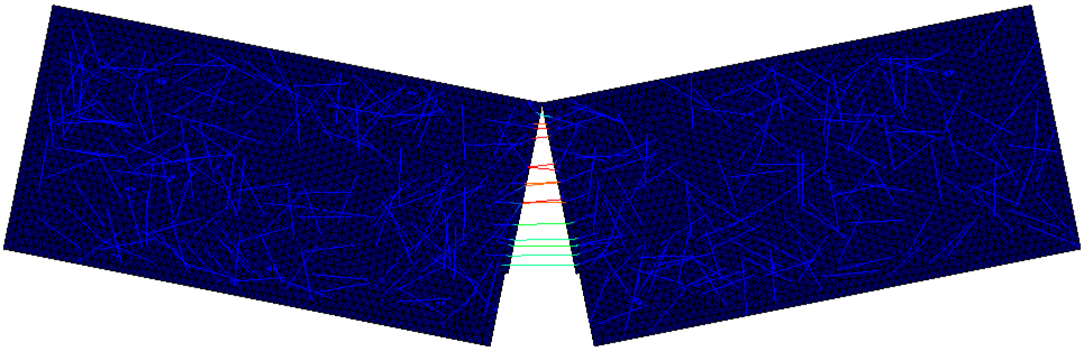

(c) Cracked configuration of the RSFRC 0-05 specimen.

Figure 4: Adopted finite element mesh, interfaces position and possible cracked configuration of the 4-point bending beam. As example there is plotted the results of the RSFRC 0-05 specimen.

Figures 5 to 8 show the numerical response in terms of vertical load vs. Crack Tip Opening Displacements (CTOD) against the corresponding experimental results. It can be observed that the proposed model leads to very accurate simulations of the post-cracking response observed in the experimental tests. As expected, the load–CTOD responses of concrete with or without fibers emphasize the significant influence of fibers on the both peak strength and post-peak response of the FRC specimens tested in bending: the brittle behavior of the concrete matrix became significantly tougher when fibers are added as spread reinforcement.

The numerical simulations, as well as the experimental observations, confirm that the post-cracking response of FRC specimens with only ISFs is characterized by the highest toughness, as a result of the superior bond properties and dowel action of these fibers with respect to RSFs.

The model formulation is also capable to capture the effect of replacing increasing amount of ISFs with an equal quantity of RSFs. Both experimental and numerical results highlight as the post-cracking behavior of FRC is generally characterized by a more pronounced softening range in specimens having a greater quantity of RSFs in substitution of ISFs. It should be noted that the local bond–slip and dowel laws were determined through inverse identification on test results obtained on specimens reinforced with only ISFs and/or RSFs. Numerical predictions of hybrid industrial/recycled steel fiber-reinforced concrete have been obtained by just changing the fiber types/contents.

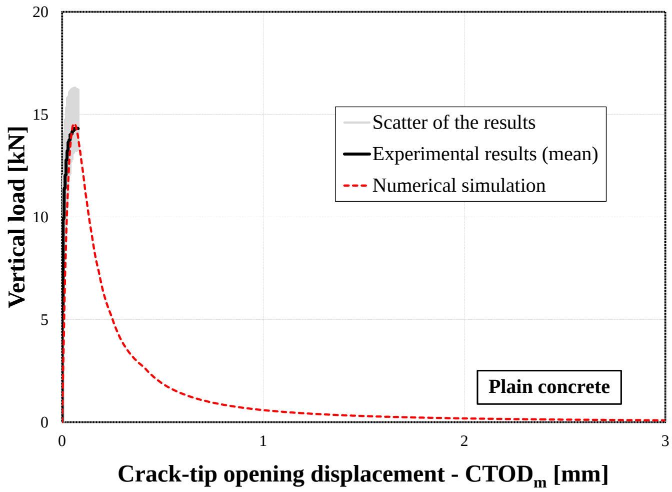

Figure 5: Vertical force – $CTOD_m$ curves of plain concrete.

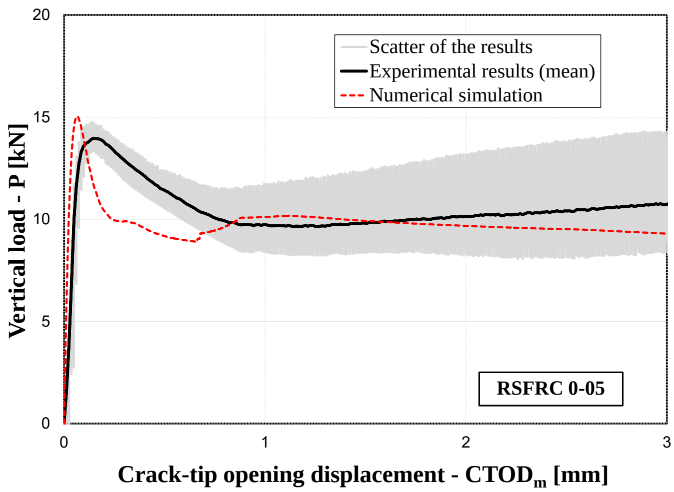

Figure 6: Vertical force – $CTOD_m$ curves of RSFRC 0-05.

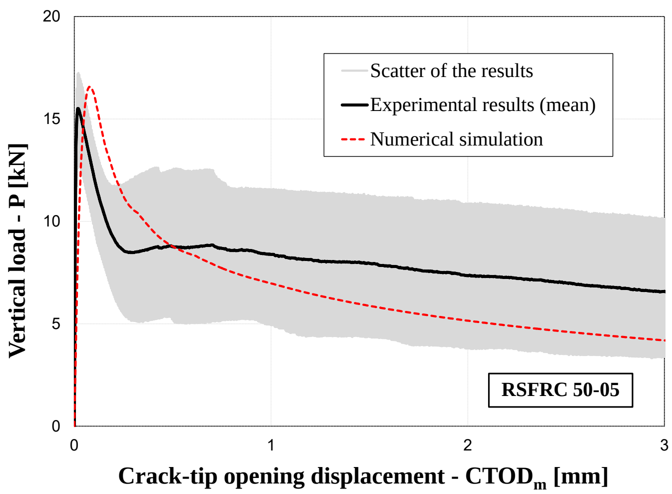

Figure 7: Vertical force – $CTOD_m$ curves of RSFRC 50-05.

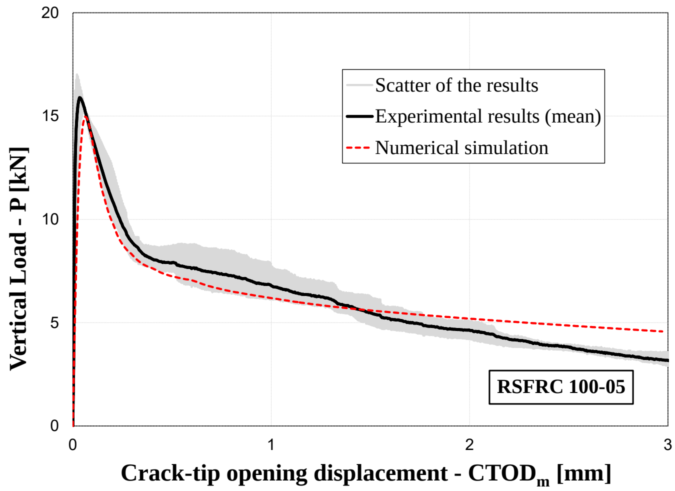

Figure 9: Vertical force – $CTOD_m$ curves of RSFRC 100-05.

6 CONCLUSIONS

This paper has presented a meso-mechanical model for simulating the fracture response of HRSFRCs in bending. It is based on a discontinuous crack finite element approach and assumes dispersed fibers “embedded” within the mesh of the cementitious matrix.

The numerical results demonstrate the capability of the proposed model in simulating the experimental observations derived by four-point bending tests on hybrid recycled/industrial steel fiber-reinforced concrete specimens. Particularly, the model is capable to capture the significant influence of steel fiber contents and types on both the maximum strength and post-peak toughness exhibited by the aforementioned specimens.

Finally, although further experimental comparisons are needed for achieving a full validation, the proposed model paves the way toward predicting the fracture behavior of HRSFRCs as a result of the mechanical properties and geometric distribution of their key constituents.

7 ACKNOWLEDGMENTS

The model proposed in this paper stems out of the activities of the SUPERCONCRETE Project (H2020-MSCA-RISE-2014, n. 645704): the Authors wish to acknowledge the financial contribution of the European Union, as part of the H2020 Programme.

REFERENCES

[1] M. Sienkiewicz, J. Kucinska-Lipka, H. Janik, A. Balas, Progress in used tyres management in the European Union: a review, *Waste Manage.* **32**(10), 1742-1751, 2012.

[2] EU-Directive1999/31/EC of the council of 26 April 1999 on the landfill of waste, *Off. J. Eur. Union L*, **182**, 1-19, 1999.

[3] E. Ganjian, M. Khorami, A.A. Maghsoudi, Scrap-tyre-rubber replacement for aggregate and filler in concrete, *Constr. Build. Mater.*, **23**(5), 1828-1836, 2009.

[4] G. Centonze, M. Leone, M. Aiello, Steel fibers from waste tires as reinforcement in concrete: a mechanical characterization, *Constr. Build. Mater.*, **36**, 46-57, 2012.

[5] A.G. Graeff, K. Pilakoutas, K. Neocleous, M.V.N. Peres, Fatigue resistance and cracking mechanism of concrete pavements reinforced with recycled steel fibres recovered from post-consumer tyres, *Eng. Struct.*, **45**, 385-395, 2012.

[6] W.H. Yung, L.C. Yung, L.H. Hua, A study of the durability properties of waste tire rubber applied to self-compacting concrete, *Constr. Build. Mater.*, **41**, 665-672, 2013.

[7] A. Caggiano, M. Cremona, C. Faella, C. Lima, E. Martinelli, Fracture behavior of concrete beams reinforced with mixed long/short steel fibers, *Constr. Build. Mater.*, **37**, 832-840, 2012.

[8] M. Elser, E. Tschegg, S. Stanzl-Tschegg, Fracture behaviour of polypropylenefibre-reinforced concrete under biaxial loading: an experimental investigation, *Compos Sci Technol*, **56**(8), 933-945, 1996.

[9] N. Banthia, F. Majdzadeh, J. Wu, V. Bindiganavile, Fiber synergy in hybrid fiber reinforced concrete (hyfrc) in flexure and direct shear, *Cem Concr Compos*, **48,** 91-97, 2014.

[10] E. Martinelli, A. Caggiano, H. Xargay. An experimental study on the post-cracking behaviour of Hybrid Industrial/Recycled Steel Fibre-Reinforced Concrete, *Construction and Building Materials*, **94**, 290-298, 2015.

[11] F. de Andrade Silva, B. Mobasher, R.D.T. Filho, Fatigue behavior of sisal fiber reinforced cement composites, *Mater Sci Eng: A*, **527**(21–22), 5507-5513, 2010.

[12] M. Nataraja, N. Dhang, A. Gupta, Stress-strain curves for steel-fiber reinforced concrete under compression, *Cem Concr Compos*, **21**(56), 383-390, 1999.

[13] A. Brandt, M. Glinicki, J. Potrzebowski, Application of FRC in construction of the underground railway track, *Cem Concr Compos*, **18**(5), 305-312, 1996.

[14] A. Caggiano, G. Etse, E. Martinelli, Zero-thickness interface model formulation for failure behavior of fiber-reinforced cementitious composites, *Comput Struct*, **98-99**, 23-32, 2012.

[15] V.M. Cunha, J.A. Barros, J.M. Sena-Cruz, A finite element model with discrete embedded elements for fibre reinforced composites, *Comput Struct*, **94-95**, 22-33, 2012.

[16] G. Etse, A. Caggiano, S. Vrech. Multiscale failure analysis of fiber reinforced concrete based on a discrete crack model. *International J of Fracture*, **178**.1-2, 131-146, 2012.

[17] A. Caggiano, E. Martinelli, A unified formulation for simulating the bond behaviour of fibres in cementitious materials, *Mater Des*, **42**, 204-213, 2012.

[18] A. Caggiano, H. Xargay, P. Folino, E. Martinelli, Experimental and numerical characterization of the bond behavior of steel fibers recovered from waste tires embedded in cementitious matrices, *Cement and Concrete Composites*, **62**, 146-155, 2015.

[19] I. Carol, P. Prat, C. Lopez, Normal/shear cracking model: applications to discrete crack analysis. *ASCE-J Engrg Mech*, **123**, 765-773, 1997.

[20] A. Caggiano, G. Etse, Coupled thermo–mechanical interface model for concrete failure analysis under high temperature. *Computer Methods in Applied Mechanics and Engineering*, **289**, 498-516, 2015.

[21] S. Vrech, G. Etse, A. Caggiano. Thermodynamically consistent elasto-plastic microplane formulation for fiber reinforced concrete. *International Journal of Solids and Structures*, **81**, 337-349, 2015.